Characterizing small-scale migration behavior of sequestered CO2 in a realistic geological fabric

GCCC Digital Publication Series #12-02

Priya Ravi Ganesh
Steven L. Bryant
T. A. Meckel

Keywords:
Modeling – Flow simulation; Capacity; Trapping mechanisms; Characterization

Cited as:
Ganesh, P. R., Bryant, S. L.; and Meckel, T. A., 2012, Characterizing small-scale migration behavior of sequestered CO2 in a realistic geological fabric: draft in review with Env. Sci. & Tech., submitted 04/01/12. GCCC Digital Publication Series #12-02.

Characterizing small-scale migration behavior of sequestered CO_2 in a realistic geological fabric

Priya Ravi Ganesh*[$], Steven L Bryant[$] and T.A Meckel[+]

[$]Department of Petroleum and Geosystems Engineering, University of Texas at Austin, 200 E. Dean Keeton Stop C0300, Austin, TX 78712-15851

[+]Bureau of Economic Geology, University of Texas at Austin, University Station, Box X, Austin, Texas 78713

ABSTRACT

For typical reservoir conditions, buoyancy and capillary forces grow dominant over viscous forces within a few hundred meters of the injection wells as the pressure gradient due to injection decreases, resulting in qualitatively different plume migration regimes. The migration regime depends on two factors: the capillary pressure of the leading edge of the plume and the range of threshold entry pressures within the rock at the leading edge of the plume. A capillary channel regime arises when these two factors have the same magnitude. Flow patterns within this regime vary from finger-like structures with minimal rock contact to back-filling structures with compact volumes of saturation distributed between fingers. Reservoir heterogeneity is one of the principal factors influencing CO_2 migration pathway in the capillary channel regime. Here we characterize buoyancy-driven migration in a natural 2D geologic domain (1 m × 0.5 m peel from an alluvium) in which sedimentologic heterogeneity has been resolved at sub-millimeter (depositional) resolution. The relevant features of the heterogeneity are grain size distribution, which determines the mean and range of threshold pressures and correlation lengths of threshold pressures in horizontal and vertical directions. The relevant physics for this migration regime is invasion percolation, and simulations indicate that CO_2 migrates through the peel in a few narrow pathways which cannot be captured by conventional coarse-grid simulations. The storage efficiency of the capillary channel regime would be low and consequently CO_2 would also migrate greater distances than expected from models or simulations that neglect the capillary channel flow regime.

INTRODUCTION

Carbon dioxide content in the atmosphere has increased considerably over the past few decades due to anthropogenic emissions. For geological storage in deep saline aquifers to mitigate atmospheric greenhouse gas content, numerous geological characterization and simulation efforts are investigating the most efficient utilization of reservoir pore volume for maximum security of storage.

Plume migration regimes

When CO_2 is injected into a storage reservoir during sequestration, viscous forces dominate flow behavior near the wellbore due to high injection rates and large pressure gradients (regime (a), Figure 1). CO_2 moves in a compact front, completely flooding all the pores it encounters in the rock. The shape of the saturation front in this near-wellbore region is determined by the spatial correlation of permeability in the storage formation.[1] As CO_2 advances into the medium farther from the injection well, the velocity of propagation of CO_2 and the pressure gradient decrease. Still farther from the injection point, the pressure gradient from injection becomes negligible[2] compared to buoyancy forces. This point is nearer the wellbore after injection ends. At this point capillary forces begin to

determine whether the meniscus between migrating CO_2 and native brine will move into a pore throat. The capillary pressure of the leading edge of the CO_2 front depends on the density difference between CO_2 and native brine ($\Delta\rho$):

$$P_c = \Delta\rho g h_{eff} + P_{inj} \quad \text{... (1)}$$

where h_{eff} is the effective height of the plume front measured vertically from the leading edge to the bottom of the continuous column of migrating CO_2 and P_{inj} accounts for the increment in P_{CO2} and P_w at the top of the plume due to injection pressure. Far from the injection well or after injection ends, $P_{inj} = 0$.

Once CO_2 is driven by buoyancy and influenced by capillarity, then a competition emerges between the CO_2 plume height (and hence the capillary pressure at the leading edge of the front) and the magnitude of the threshold pressures P_{th} in the reservoir rock.[3] Generically three possible outcomes exist for this competition, yielding flow regimes (a), (b) and (c) in Figure 1. In flow regime (a), $P_c > \max(P_{th})$, i.e. the capillary pressure exceeds the maximum threshold pressure of the reservoir rock and *compact flow* of CO_2 occurs (i.e. CO_2 enters every pore throat it encounters). This would be a continuation of the near-wellbore migration regime. In flow regime (b) $\min(P_{th}) < P_c < \max(P_{th})$, i.e. the CO_2 capillary pressure is greater than the smallest threshold pressure but does not exceed the highest threshold pressure in that portion of the reservoir rock. The CO_2 migration pattern adopts a *capillary channel* structure characteristic of invasion percolation where the direction of invasion is vertically biased due to buoyancy. Because CO_2 migrates through much less of the rock volume in this regime, a given mass will migrate much farther than in compact flow, with important consequence for CO_2 storage.[4-7] In flow regime (c) where the capillary pressure is smaller than the minimum threshold pressure of a *seal rock*, i.e. $P_c < \min(P_{th}^{seal})$, further migration of the plume is blocked or redirected. If CO_2 cannot migrate around this barrier, it will accumulate with progressively increasing P_c similar to natural reservoirs of hydrocarbon or CO_2.

The competition between capillary pressure and threshold pressure exhibits rich dynamics[8-10] for three reasons: 1) the contribution of injection pressure to P_c (Equation 1) varies with distance from the injection well and with time; 2) the plume height (h_{eff}) and hence P_c varies with distance traveled especially once injection ceases and subsequent migration leaves residual CO_2 saturation behind; and 3) spatial heterogeneity in the petrophysical properties (P_{th}) of the storage formation. The three flow regimes have very different implications for the extent of plume migration and for storage efficiency. Thus it is important for simulations of sequestration to capture these various regimes. Compact flow is familiar from the coarse-grid simulations commonly applied to storage at the reservoir-scale (e.g. Eclipse, GEM); these simulations typically neglect capillary pressure. The influence of seals is also familiar, though usually encountered as a region of very small or zero permeability imposed on the domain, rather than as a capillary barrier. In contrast to compact flow and secondary accumulation beneath a seal, capillary channel flow is observed only if the simulation accounts explicitly for the heterogeneous distribution of threshold pressures of the rock.[8]

Below we present simulations of CO_2 migration and displacement pattern for the capillary channel flow regime ((b) in Figure 1). To simplify the presentation, we assume an infinite source of CO_2 far from the

displacement front (mimicking a continuous injection site) that feeds buoyant CO_2 with sufficient capillary pressure to migrate through the portion of a reservoir represented by our geologic specimen.

Modeling the physics of capillary channel flow

The basic physics of buoyant migration of the non-wetting CO_2 phase through a heterogeneous domain is an extension of invasion percolation. The key rule governing invasion percolation is that if the capillary pressure exceeds the threshold pressure of the pore throat, then nonwetting fluid passes through the throat and enters the adjoining pore; otherwise the pore throat continues to act as a barrier.

Our application is closely related to basin analysis, which explores migration of hydrocarbons generated at depth and migrating toward potential traps. Basin analysis identifies traps and potential leads and prospects in the area likely to have received hydrocarbons. While basin modeling is performed on a large scale, buoyancy and capillary forces acting over small domains are still the main drivers influencing hydrocarbon migration.

We use the commercial software Permedia® (formerly MPath), a modified invasion percolation based simulator distributed by Halliburton, to investigate the buoyant rise of CO_2. We assume CO_2 enters from a line source at the bottom boundary of the domain. The domain is given periodic lateral boundaries to eliminate boundary effects and artificial upward bias in plume migration for all simulation cases. A simulation terminates when rising CO_2 reaches the top boundary of the domain. The digitally-represented model is derived from a natural geologic specimen with highly resolved (mm-scale) spatial heterogeneity represented by depositional fabric, described below.

Heterogeneous geologic domain

The model domain is a digital representation of a physical geologic specimen. The specimen (Figure 2(a)) is a vertically-oriented, quasi-2D sedimentary relief peel sample (1.0 m × 0.5 m) of fluvial sediment extracted from the upper portions of a modern point bar of the Brazos River, Texas[11,12]. The specimen broadly consists of cm-scale ripple-laminated well-sorted lower-fine to lower-very-fine sand. Topographic relief of the sample surface reflects varying extent of imbibition of viscous fluid (epoxy) used for sample preparation and thus correlates with key petrophysical properties.[13] The high-resolution digital elevation map obtained through laser range scanning (Figure 2(b)) indicates that peel topography is linearly correlated with variations in measured grain size (in mm) and sorting. Higher elevations correspond with greater imbibitions as a result of smaller average grain size (hotter colors, Figure 2(b)) and lower elevations correspond with lesser imbibition as a result of larger average grain size (cooler colors, Figure 2(b)).

We use this elevation data as a proxy for rock property of interest here, namely, threshold entry pressure for drainage (invasion of CO_2). Values of threshold pressure calculated from the measured grain size distribution were assigned to grid elements by assuming the simple Berg equation[14] (1975) applies for CO_2- H_2O system.

$$P_c^{threshold} = P_{th} = 16.3 \times \frac{IFT}{D\_mm} \qquad \ldots (2)$$

The geologic model used for simulation is a representation of the heterogeneity of this sample as shown by the calculated threshold

pressure map in Figure 2(c) using equation 2. This threshold pressure map is similarly color coded with red shades implying regions of highest threshold pressure that correspond to highest elevations in the domain as shown. For presentation of simulation results, the threshold pressure maps shows lighter gray shades in the grayscale domain background corresponding to high P_{th} (high elevations [red] in original topography dataset). A concise representation of the model development process[15] is given in Figure 2.

SIMULATION OF CAPILLARY CHANNEL FLOW IN HETEROGENEOUS SAND

In this section we simulate buoyancy-driven migration of CO_2 in the peel model for the capillary channel migration regime. Maximum and minimum threshold pressure values of 6.1 to 8.9 kPa (mean of 7.4 kPa) are assigned to the model corresponding to the minimum and maximum grain sizes of 0.055 and 0.08 mm determined for the specimen. CO_2 fingers migrate preferentially through regions of lower threshold pressure which have an architecture defined by the depositional fabric. The CO_2 occasionally forms small accumulations below the light gray patches corresponding to barriers having highest threshold pressures in the domain (Figure 3). The percentage of the domain saturated with CO_2 is 2.86%, which is quite small. These capillary channels efficiently transport all CO_2 that enters the domain through a few narrow, generally vertical pathways.

EFFECT OF HETEROGENEITY ON CAPILLARY CHANNELS

The migration behavior in Figure 3 is specific to that geologic specimen and the assumed height of the CO_2 plume entering the specimen. Now we examine the effect of different degrees of heterogeneity on the migration of CO_2.

Case 1: Effect of threshold pressure range on CO_2 migration regime

In this series of simulations we keep the peel fabric (correlation structure of depositional sedimentary fabric) the same but change the assigned values (ranges and magnitudes) of threshold pressure. The threshold pressure range and magnitude depend on grain size distribution, so this exercise does not strictly adhere to a sedimentologically accurate relationship between depositional fabric, grain size, and threshold pressure. However it does provide insight into how such fabrics may influence flow in rocks with different petrophysical properties. We use a 0.1 m × 0.1 m subsection (250000 cells) of the peel model to resolve CO_2 migration patterns at native depositional resolution while systematically varying the range of threshold pressures (Table 1).

Threshold pressure range here is defined as the difference between the maximum and minimum values of threshold pressure. We use with standard deviations of 0.02, 0.2 and 0.4 kPa about the mean threshold pressure, which is held fixed at 7.4 kPa. Wider ranges of threshold pressure imply more heterogeneity, e.g. poorer sorting or wider grain size distributions, while narrower threshold pressure ranges suggest more homogeneous or well-sorted domains.

In this fixed depositional fabric, CO_2 migration in capillary channels exhibits a transition from fingering to back-filling pattern as grain size distribution widens in the domain (Figure 4). In an extremely well-sorted rock (left panel, Figure 4) CO_2 encounters few capillary barriers due to the narrow range of threshold pressure

distribution. Poorer sorting (middle and right panels, Figure 4) reduces efficiency of CO_2 migration through the domain and back-filling occurs as some regions in the domain act as local flow barriers. Thus storage efficiency reduces as buoyancy and heterogeneity in extremely well-sorted reservoirs enable much CO_2 to finger long distances with minimal rock contact volume. Though back-filling in moderately sorted reservoirs comparatively increases storage efficiency, CO_2 still occupies much lesser volume than nominal storage capacity.

While certain values of threshold pressure may not be practically applicable for the physical sedimentary specimen we possess, these ranges nonetheless could represent other depositional environments. For example, very narrow threshold pressure ranges could signify engineered sandpacks and higher threshold pressure ranges could be in typical sandstone reservoirs with poorly sorted grains of sand and silt. Indeed migration experiments on sandpacks show CO_2 migrating in preferential paths in the form of fingers through the medium.[16]

Case 2: Effect of correlation length of threshold pressures on CO_2 migration regime

Case 2 maintains the threshold pressure field (range and values) but varies spatial correlation of P_{th}. From case 1 we select the threshold pressure range of 6.3 - 8.9 kPa (Figure 4, middle panel) and study the effect of varying the underlying structure (fabric) of the domain on CO_2 migration using geostatistical realizations of different horizontal and vertical correlation lengths of threshold pressures (Figure 5).

Qualitatively, extensive fingering occurs at longer vertical correlation lengths while longer horizontal correlation lengths enhance CO_2 back-filling. The ratio of horizontal and vertical correlation lengths of threshold pressures in the domain influences the size of CO_2 accumulations (Figure 5a and 5b). The higher the ratio (right panel, Figure 5a and left panel, Figure 5b), the greater the tendency of CO_2 to back-fill and thus contact more rock as it migrates. This reiterates the importance of the underlying fabric in influencing CO_2 migration regime. It is worth mentioning that no back-filling occurs in domains with randomly distributed P_{th} values and we find fine CO_2 stringers in uncorrelated fields.[8]

RESULTS AND DISCUSSION

As we simulate various degrees of heterogeneity in our peel (ranges of P_{th}), we observe a transition of CO_2 migration between predominantly fingering and predominantly back-filling patterns.[17] The fingering pattern exhibits structures of narrow, mostly vertical, preferential flow paths that yield a very small average saturation of CO_2 in the domain. The back-filling pattern has numerous regions completely filled with CO_2, and each region is usually connected to a small number of neighboring regions by narrow flow paths, yielding a larger average saturation. When capillary pressure of the leading edge of the CO_2 plume is either greater or lesser than the threshold pressure range of the reservoir section it encounters, we observe the compact flow regime or the secondary accumulation regime respectively, both of which are adequately represented by conventional simulation techniques. The capillary channel flow regime occurs wherever buoyancy drives the CO_2 migration, i.e. in most of the reservoir, and where the plume height is not too large. For typical storage conditions the capillary pressure gradient within a CO_2 plume is about 0.1 psi/ft. Thus for typical storage formations the limit on continuous

plume height would range from around ten feet in high permeability/high porosity sands (entry pressures similar to those of the peel) to hundreds of feet in low permeability rock (e.g. 140 ft plume height for 10 mD Mt Simon sandstone in Central Illinois). Plume heights exceeding this limit will exhibit compact flow, while plume heights much smaller than this limit will lead to secondary accumulation. Thus the broader the distribution of threshold pressures, the greater the likelihood of capillary channel flow.

If CO_2 migration through a major portion of the reservoir is in the capillary channel regime, the storage efficiency potentially much smaller. If the migration pattern tends towards fingering then the storage capacity would be much less than the nominal value (rock pore volume), because CO_2 fingers through so small a cross-section of the rock. The back-filling pattern builds a large saturation in more of the pore volume, but still considerably less than the nominal storage capacity. More spatial correlation[18,19] and wider grain size distributions are conducive for the back-filling migration pattern. With more compact and thus less efficient plume migration pathways, these make preferred storage sites. This is necessary to be modeled because if we assume the peel fabric to represent a typical storage reservoir, simulations indicate that CO_2 migrates through the peel in a few narrow pathways which cannot be captured by conventional coarse-grid simulations. CO_2 would migrate greater distances than expected from models or simulations that neglect the capillary channel flow regime. This would continue until CO_2 encounters a 'barrier' it cannot penetrate through due to insufficient driving capillary pressure of the leading edge of the mobile front. Fingering would thus not be preferable considering the motivation behind sequestration as the storage efficiency in the capillary channel regime would be extremely low.

The dynamics of capillary channel flow with possible migration patterns from fingering to back-filling cannot be captured by standard continuum simulators with large (meter scale) grid elements to which a single "average" capillary pressure curve and set of relative permeability curves must be assigned. CO_2 observed to migrate vertically through shaly horizons in the Utsira formation is an interesting case of flow through what are usually considered to be barriers.[20] In Utsira, CO_2 accumulations are found to grow laterally beneath each shale layer and also penetrate vertically through them which cannot be predicted as such by conventional simulation models. Modeling the dominant flow physics at the appropriate scale is thus important to get valid estimates of fluid migration through formations and effective storage capacity. Typical simulations with geologically unrepresentative (i.e. large yet homogeneous) grid blocks cannot capture this range of behavior and thus yield optimistic estimates of the amount of CO_2 saturating a region and the distance travelled by a buoyant plume.

CONCLUSION

The capillary channel migration regime occurs in heterogeneous storage formations when the capillary pressure at the leading edge of a CO_2 plume is comparable to the range of threshold pressures in the rock. In this regime, flow patterns vary from fingering structures with minimal rock contact to back-filling with locally compact saturation distribution as the degree of heterogeneity increases. High-resolution (sub-millimeter) characterization of a geologic specimen enables simulation of the physics relevant in this regime (invasion percolation) at the relevant scale, and a predominantly fingering migration pattern is predicted. Compared to the compact flow

regime, the capillary channel regime yields small storage efficiency and consequently would result in CO_2 migration over longer distances. The significance of getting the dominant flow physics right is amplified as these fine fingers of CO_2 create very small average saturations that would not show up on seismic analysis.[6,19-21] Hence, we must rightly account for percolation processes in non-viscous domains which is not possible by conventional finite-difference simulators.

The results emphasize that the depositional fabric and the degree of reservoir heterogeneity can significantly affect plume migration. Incorporating percolation effects due to reservoir heterogeneity at the appropriate scale in the simulation model is thus essential to realistically qualify plume migration patterns affecting the efficiency of the storage reservoir. We have currently applied this analysis to one geologic facies, and hope to include others in future.

ACKNOWLEDGEMENTS

The authors gratefully acknowledge funding from NETL CCS characterization project (DE-FE0001941). Thanks also to the Gulf Coast Carbon Center and Bureau of Economic Geology at The University of Texas at Austin for providing generously for both facilities and support for the execution of this work.

REFERENCES

(1) Bryant, Steven L.; Lakshminarasimhan, Srivatsan; Pope, Gary A. Buoyancy-dominated multiphase flow and its effect on geological sequestration of CO_2. SPE 99938, December 2008.

(2) Kumar, Navanit. CO2 sequestration: Understanding the plume dynamics and estimating the risk. Master's Thesis, Department of Petroleum Engineering, The University of Texas at Austin, 2008.

(3) Auradou H; Maloy, Knut Jorgen; Schmittbuhl, Jean; Hansen A; Bideau D. Competition between correlated buoyancy and uncorrelatated capillary effects during drainage. Physical Review E 1999, 60 (6), 7224-34.

(4) Carruthers, Daniel J.F. Transport modelling of secondary oil migration using gradient-driven invasion percolation techniques. Ph.D. Dissertation, Department of petroleum Engineering, Heriot-Watt University, Edinburgh, Scotland UK, 1998.

(5) Krevor, Samuel C.M.; Pini, Ronny; Li, Boxiao; Benson, Sally M. Capillary heterogeneity trapping of CO2 in a sandstone rock at reservoir conditions. Geophysical Research Letters, 2011, 38, L15401; DOI:10.1029/2011GL048239.

(6) Luo, X.R.; Zhou, B.; Zhao, S.X., Zhang, F.Q; Vasseur, G. Quantitative estimates of oil losses during migration, part I: the saturation of pathways in carrier beds. Journal of Petroleum Geology, 2007, 30(4), 375-387.

(7) Ringrose, P.S.; Corbett, P.W.M. Controls on two-phase fluid flow in heterogeneous sandstones. Geofluids: Origin, Migration and Evolution of fluids in Sedimentary Basins, Geological Society Special Publication, 1994, 78, 141-150.

(8) Saadatpoor, Ehsan; Bryant, Steven L.; Sepehrnoori, Kamy. New trapping mechanism in carbon sequestration. Trans. Porous Media, 2009, 82, 3-17.

(9) Singh, Varunendra; Cavanaugh, Andrew; Hansen, Hilde; Nazarian, Bamshad; Iding, Martin; Ringrose, Philip. Reservoir modeling of CO2 plume behavior calibrated against monitoring data from Sleipner, Norway. Paper 134891 presented at the SPE Annual Technical Conference and Exhibition held in Florence, Italy, 19-22 September 2010.

(10) Zhang, Changyong; Oostrom, Mart; Wietsma, Thomas W.; Grate, Jay W.; Warner, Marvin G. Influence of viscous and capillary forces on immiscible fluid displacement: pore-scale experimental study in a water-wet micromodel demonstrating viscous and capillary fingering. Energy Fuels; DOI:10.1021/ef101732k.

(11) Bernard, H.A., and Major, C.F., Jr., 1963, Recent meander belt deposits of the Brazos River: An alluvial “sand” model: AAPG Bull., 47(2): 350.

(12) Bernard H.A., Major, C.F., Jr., Parrott, B.S., and Le Blanc, R.J., Sr. Recent sediments of southeast Texas: A field guide to the Brazos alluvial and deltaic plains and the Galveston barrier island complex, 1970, The University of Texas at Austin, Bureau of Economic Geology, Guidebook 11.

(13) McMullen, R.M. and Allen, J.R.L. Presentation of sedimentary structures in wet unconsolidated sands using polyester resins, Marine Geol., 1964, 1:88-97.

(14) Berg, R.R. Capillary pressures in stratigraphic traps. AAPG Bull., 1975, 59(6), 939-956.

(15) Meckel, T.A. Digital modeling of a sedimentary-relief peel: implications for clastic facies characterization and fluid migration simulation, 2012, Paper in review.

(16) Glass, Robert J.; Conrad, Stephen H.; Peplinski, William. Gravity-destabilized nonwetting phase invasion in macroheterogeneous porous media: Experimental observations of invasion

dynamics and scale analysis. Water Resources Research, November 2000, 36(11), Pages 3121-3137.

(17) Cottin, Christophe; Bodiguel, Hugues; Colin, Annie. Drainage in two-dimensional porous media: From capillary fingering to viscous flow. Physical Review E, 2010, 80, 046315; DOI:10.1103/PhyRevE.82.046315.

(18) Ide, S.Taku; Jessen, Kristian; Orr Jr., Franklin M. Storage of CO2 in saline aquifers: Effects of gravity, viscous and capillary forces in amount and timing of trapping. Int. Journal of Greenhouse Gas Control, 2007, 481-491; DOI:10.1016/S1750-5836(07)00091-6.

(19) Salomao, M.C. Analysis of flow in spatially correlated systems by applying the percolation theory. Paper 39039 presented at the fifth Latin American and Caribbean Petroleum Engineering Conference and Exhibition held in Rio de Janeiro, Brazil, 30 August - 3 September 1997.

(20) Hermanrud, Christian; Teige, Gunn Mari Grimsmo; Iding, Martin; Eiken, Ola'Rennan, Lars; Ostmo, Svend. Differences between flow of injected CO2 and hydrocarbon migration. Petroleum Geology Conference series 2010, 7, 1183-1188; DOI:10.1144/0071183.

(21) Luo, X.R.; Yan, J.Z; Zhou, B.;Hou, P; Wang, W.; Vasseur, G. Quantitative estimates of oil losses during migration, part II: measurement of the residual oil saturation in migration pathways. Journal of Petroleum Geology, 2008, 31(2), 179-190.

(22) Saadatpoor, Ehsan; Bryant, Steven L.; Sepehrnoori, Kamy. CO2 leakage from heterogeneous storage formations. Paper 135629 presented at the SPE Annual Technical Conference and Exhibition held in Florence, Italy, 19-22 September 2010.

LIST OF TABLES

Values used / Cases	Density difference between CO_2 and formation brine ($\Delta\rho$)	Threshold pressure range	Correlation length of threshold pressures	Model scale (L × H)
2D peel from alluvium	300 kg/m^3 i.e. Brine density: 1000 kg/m^3 CO_2 density: 700 kg/m^3	2.8 kPa i.e.6.1- 8.9 kPa	Peel structure	1.0 m × 0.5 m
CASE 1 (see text)		0.2 - 6.1 kPa	Peel structure	0.1 m × 0.1 m
CASE 2 (see text)		2.6 kPa i.e.6.3–8.9 kPa	*Geostatistical realizations* a) Horizontal correlation length/ vertical correlation length = 10 for horizontal correlation length = 1× ,10× and 100× cell height b) Horizontal correlation length/ vertical correlation length = 10, 1, 0.1 for horizontal correlation length = 100× cell height	0.12 m × 0.12 m

Table 1: Parameter values considered for simulation cases

LIST OF FIGURES

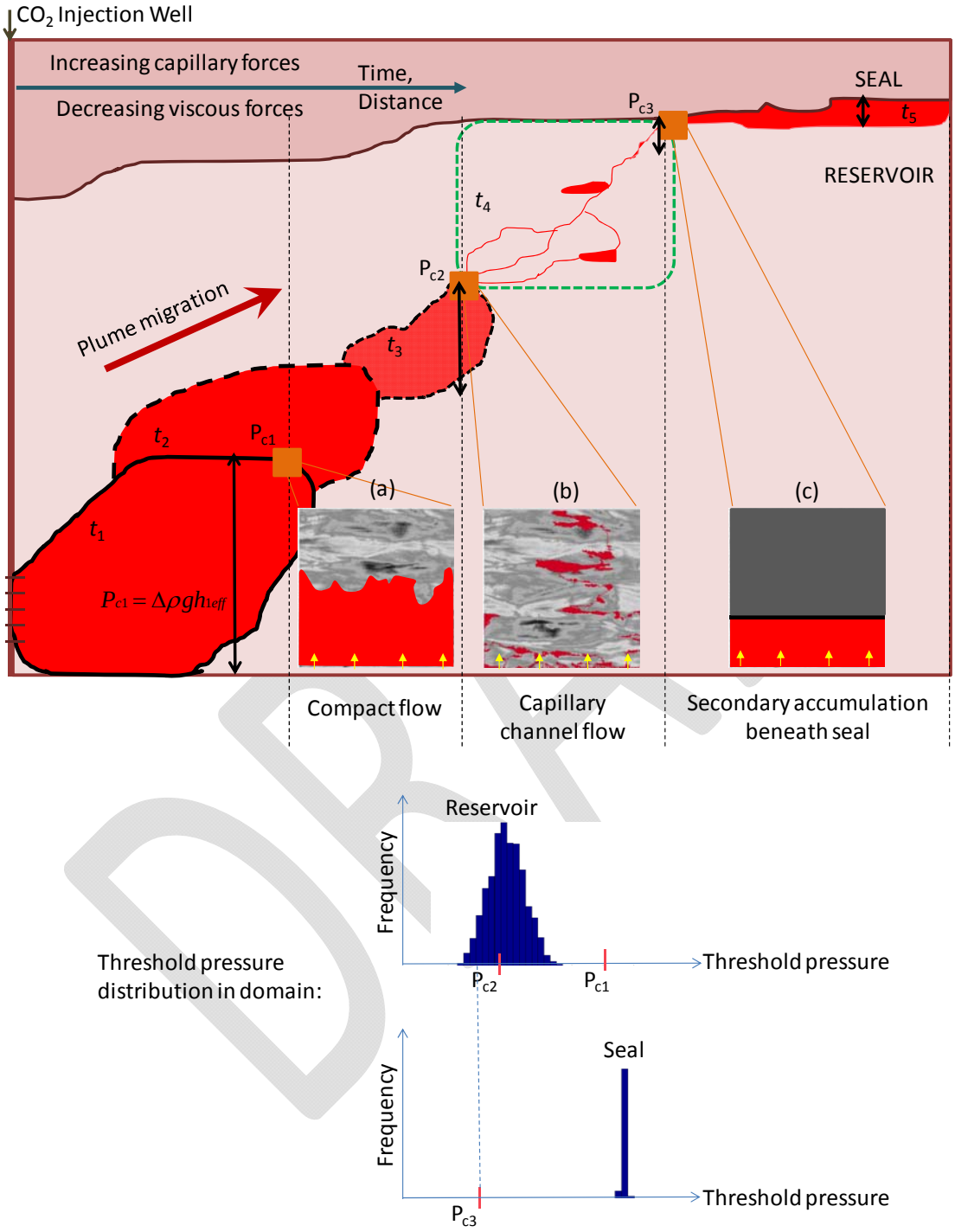

Figure 1: Schematic of spatial and temporal evolution of flow regimes from viscous-dominated to buoyancy/capillarity-dominated. As the mass of mobile CO_2 plume moves through time (outlines of plume at times t_1, t_2, t_3, t_4 and t_5 are shown) and distance in the reservoir (extreme vertical exaggeration), possible flow regimes are: (a) *compact flow* where $P_{c1} > \max(P_{th})$, where

P_{th} is the capillary entry pressure for CO_2 to enter a volume of rock; in the reservoir P_{th} has a frequency distribution shown at the bottom of the diagram, (b) *capillary channel flow* where $\min(P_{th}) < P_{c2} < \max(P_{th})$ and (c) *secondary accumulation beneath a seal* where $P_{c3} < \min(P_{th}^{seal})$. The seal rock is a different rock type with very high threshold pressure values P_{th}^{seal} compared to the reservoir rock. In this paper, we explore flow regime (b).

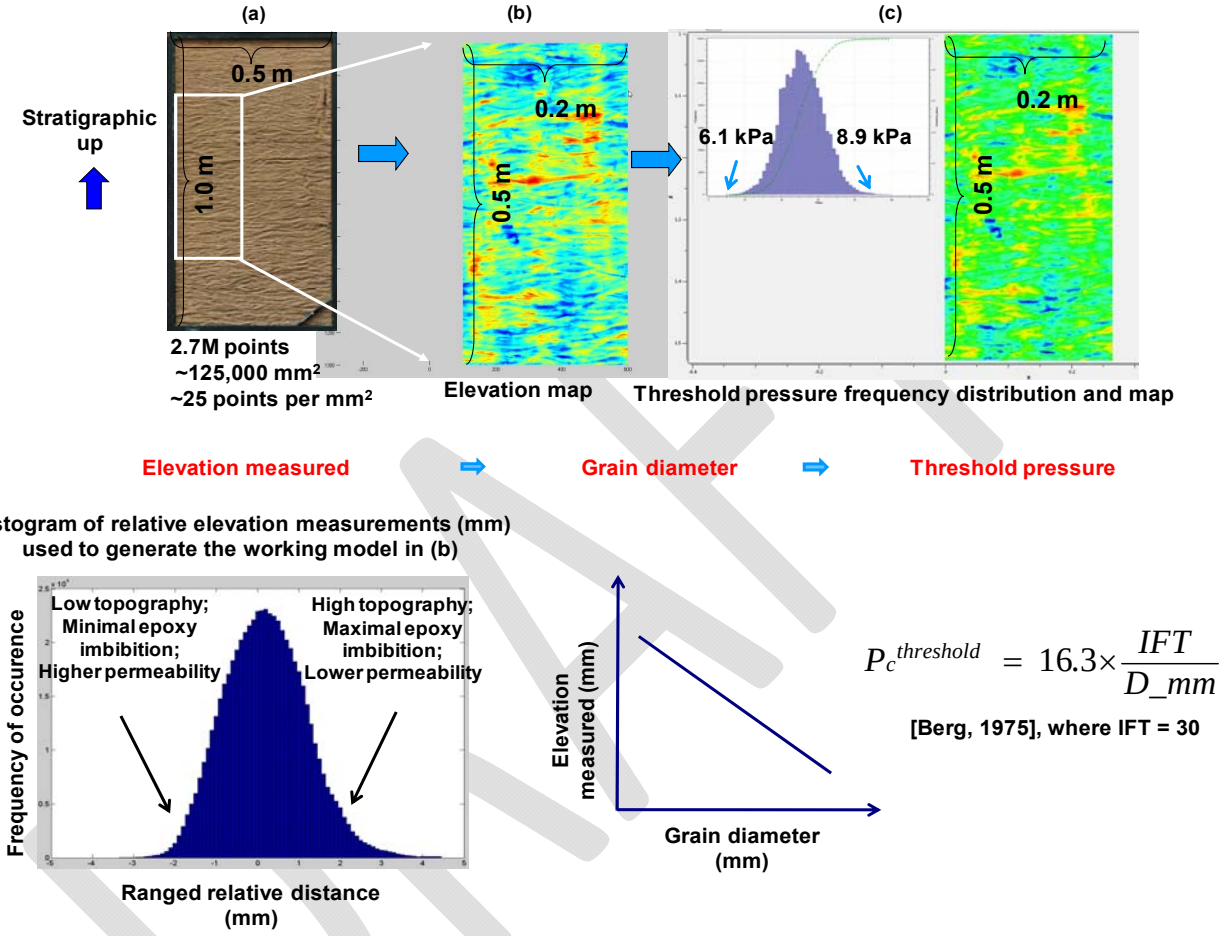

Figure 2: Summary of the geologic model. Optically ranged topography and grain diameter measurements on a 1 m by 0.5 m peel from a river alluvium are used to build high-resolution geologic model populated with threshold pressure values. Sequential stages of building the digital model are: (a) Obtained peel specimen subjected to high-resolution laser scanning and imaging techniques to study epoxy imbibition and grain size distribution; (b) Preparing digital elevation map derived from topographical variations in the peel due to epoxy imbibition; (c) Digital high-resolution model generated representing the threshold pressure distribution of the model domain corresponding to the determined topography. Details are provided in Meckel[15] (in review).

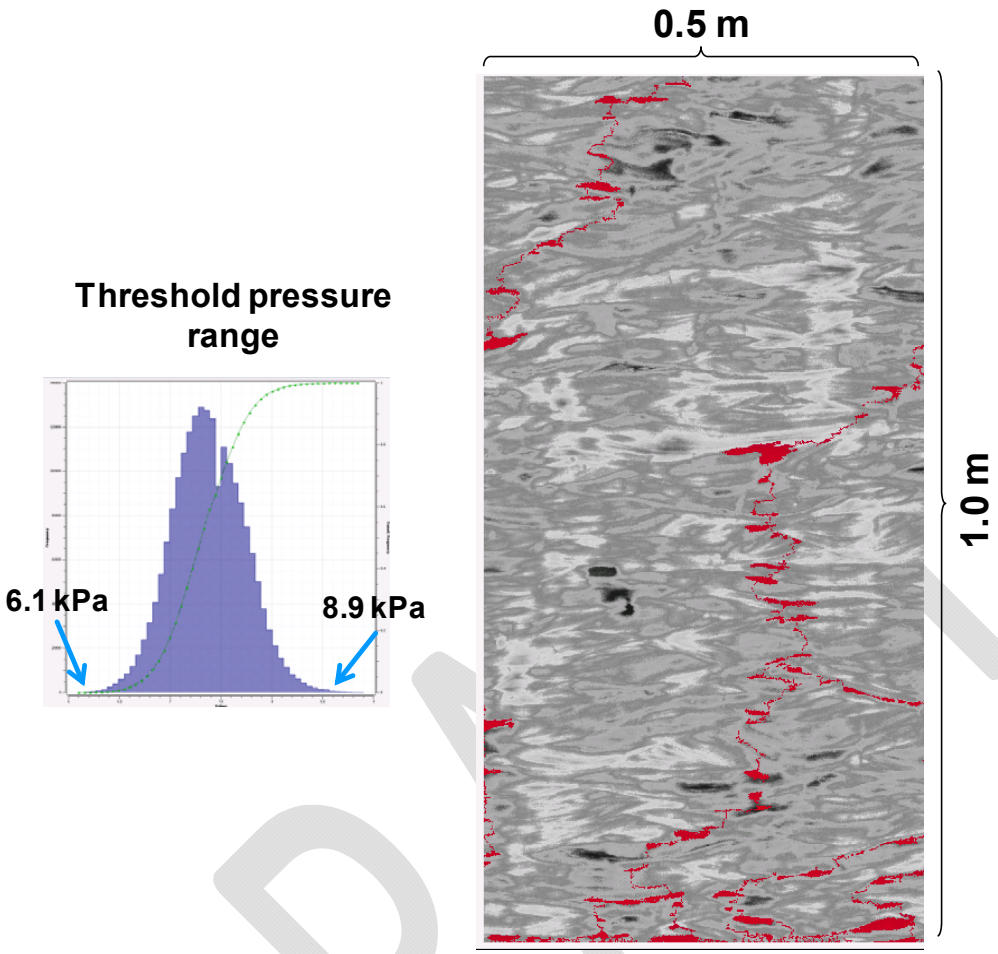

Figure 3: Invasion percolation simulation of CO_2 migrating through the peel model. Continuous line source was placed at bottom boundary of model domain, left and right boundaries are periodic. The CO_2 flow pattern is characterized as 'fingering'. 2.86% of the model domain is saturated with CO_2 at percolation.

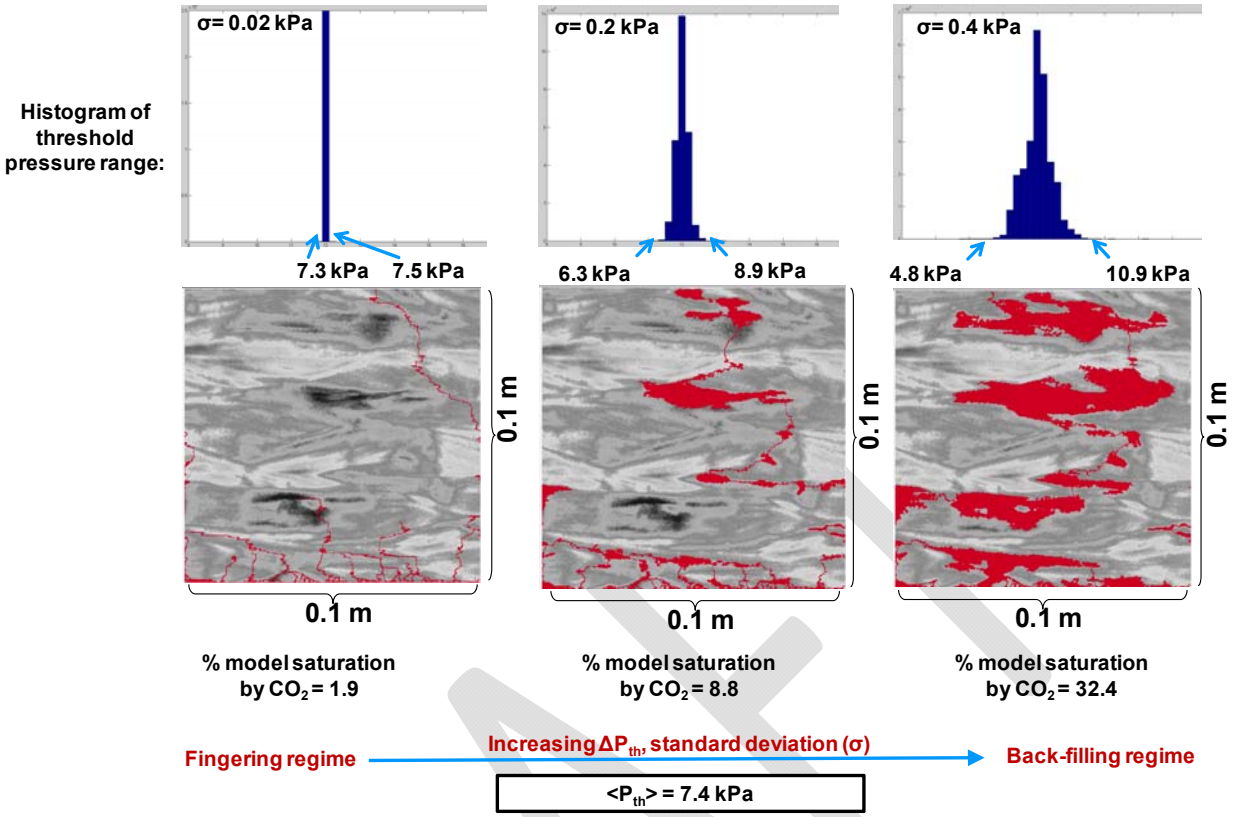

Figure 4: Flow transition from fingering to back-filling patterns occurs with increasing threshold pressure range. Mean P_{th} in all simulations is 7.4 kPa. Domains with wider grain size distribution cause CO_2 to back-fill beneath contiguous regions of larger entry pressure (light shading in background P_{th} map), so a higher percentage of the domain becomes saturated with CO_2.

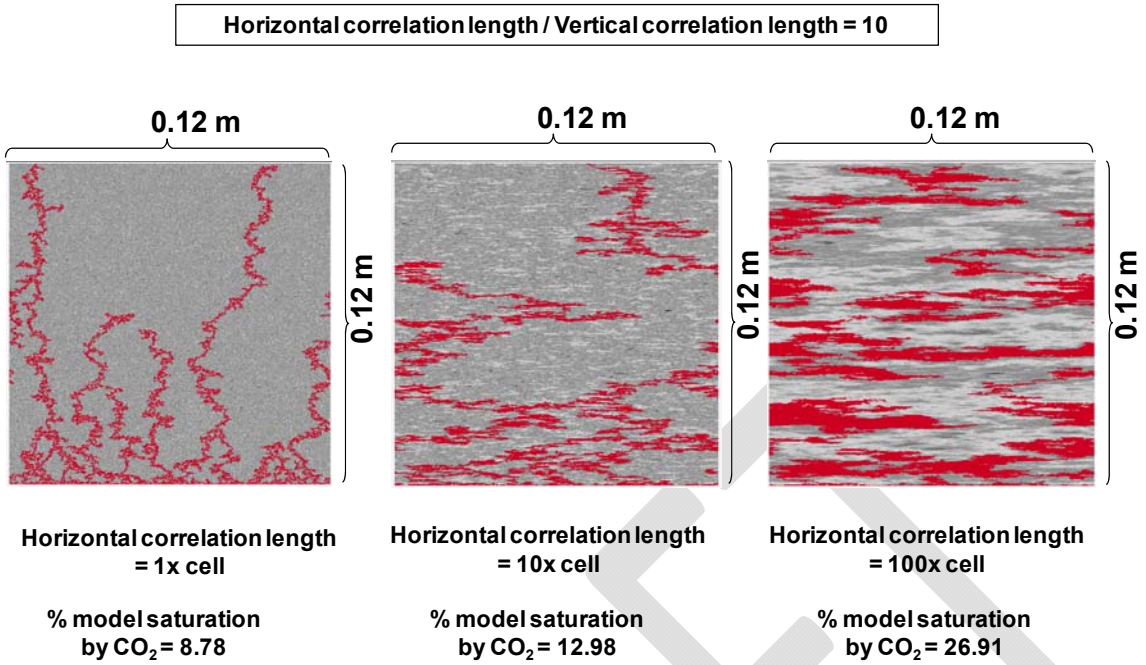

Figure 5a: Effect of ratio of horizontal and vertical correlation lengths of threshold pressure with respect to cell dimensions (2.34 mm × 2.34 mm) in the model on CO_2 migration pattern

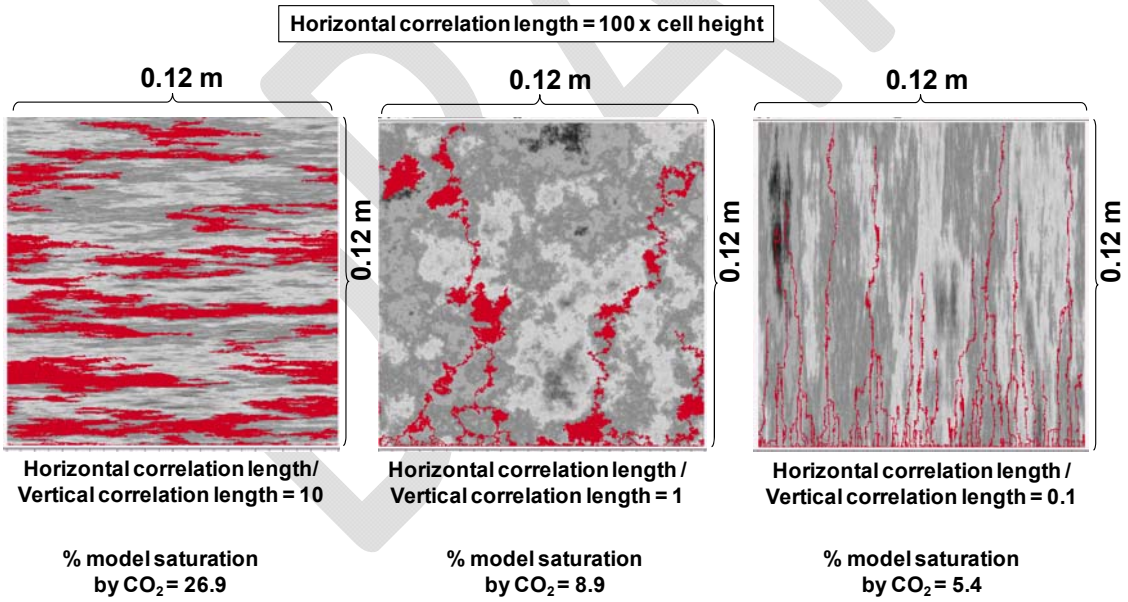

Figure 5b: Effect of ratio of horizontal and vertical correlation lengths of threshold pressure (horizontal correlation length = 100 × constant cell dimensions in the model) on CO_2 migration pattern. Higher ratios of horizontal and vertical correlation lengths in the domain lead to more lateral movement of CO_2 with increasing size of accumulations.